

DINOv2-powered Few-Shot Semantic Segmentation: A Unified Framework via Cross-Model Distillation and 4D Correlation Mining

Wei Zhuo^{1,2} Zhiyue Tang¹ Wufeng Xue^{3*} Hao Ding¹ Linlin Shen^{1,2,4*}

¹ School of Artificial Intelligence, Shenzhen University, Shenzhen 518060, China

² National Engineering Laboratory of Big Data System Computing Technology, Shenzhen University

³ School of Biomedical Engineering, Shenzhen University Medical School, Shenzhen University

⁴ School of Computer Science and Software Engineering, Shenzhen University

weizhuo@szu.edu.cn; xuewf@szu.edu.cn; llshen@szu.edu.cn; tangzhiyue2023@email.szu.edu.cn

Abstract

Few-shot semantic segmentation has gained increasing interest due to its generalization capability, i.e., segmenting pixels of novel classes requiring only a few annotated images. Prior work has focused on meta-learning for support-query matching, with extensive development in both prototype-based and aggregation-based methods. To address data scarcity, recent approaches have turned to foundation models to enhance representation transferability for novel class segmentation. Among them, a hybrid dual-modal framework including both DINOv2 and SAM has garnered attention due to their complementary capabilities. We wonder “can we build a unified model with knowledge from both foundation models?” To this end, we propose FS-DINO, with only DINOv2’s encoder and a lightweight segmenter. The segmenter features a bottleneck adapter, a meta-visual prompt generator based on dense similarities and semantic embeddings, and a decoder. Through coarse-to-fine cross-model distillation, we effectively integrate SAM’s knowledge into our lightweight segmenter, which can be further enhanced by 4D correlation mining on support-query pairs. Extensive experiments on COCO-20i, PASCAL-5i, and FSS-1000 demonstrate the effectiveness and superiority of our method.

1. Introduction

Semantic segmentation, which makes pixel-wise class prediction, has gained great success. These methods, however, typically require massive training on a large amount of densely annotated images. To avoid laborious annotation, few-shot semantic segmentation has attracted increased attention in recent years. In contrast to traditional seman-

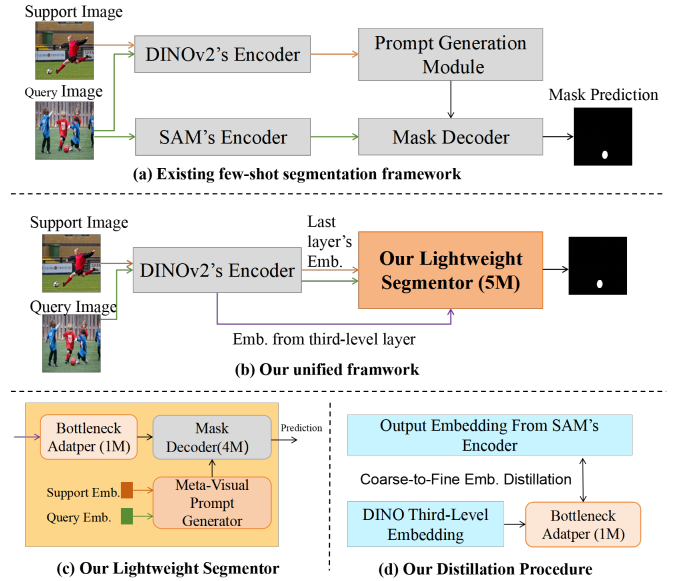


Figure 1. **Introduction of our framework.** Our framework (b) is unified and efficient compared to existing dual-modal architecture [14, 29, 37] shown in (a). Our lightweight segmenter (c) contains only 5M parameters, but gains knowledge from the powerful SAM via the procedure in (d). Note that the meta-visual prompt generator based solely on dense cosine-similarity map takes negligible parameters.

tic segmentation, few-shot semantic segmentation aspires to establish a more general framework that requires only a handful of labeled images from novel classes for segmentation.

Inspired by [28], early few-shot semantic segmentation (FSSS) methods [26, 31] employ meta-learning to mimic the inference process, learning generalized matching models through extensive meta-tasks constructed from support-query pairs of base categories. These models can be di-

*Corresponding author

rectly applied to segment novel classes without fine-tuning during inference. To enable effective support-query matching, both prototype-based [13, 36, 38, 41] and aggregation-based [7, 8, 18, 23, 39] methods are extensively exploited. Despite this, FSSS still heavily suffers from the inherent limitation of data scarcity.

Recent FSSS methods based on foundation models [1, 9, 21, 25] effectively mitigate the data scarcity limitation. This is mainly attributed to the expressive and transferable visual representations from these foundation models, which are learned on large-scale datasets. DINO [1] and DINOv2 [21] gain more attention since their embeddings highly respect local correlations and are particularly suitable for few-shot segmentation [17]. In recent years, the emergence of SAM [9], an iterative class-agnostic segmentation method, has spurred a new branch of SAM-based FSSS methods [6, 14, 37, 40]. Despite SAM’s versatility, [14, 37] found its dense features are insufficient for distinguishing various semantics, leading to hybrid FSSS frameworks combining SAM and DINOv2. Specifically, these methods leverage DINOv2 to extract local features on both support and query images for prompt generation, and then employ SAM for mask prediction. However, the dual-modal architecture (DINOv2+SAM) incurs substantial computational overhead. Training-free solutions [14, 37] exacerbate memory demands and remain sensitive to hyperparameters due to their reliance on the largest model variants and complex manual processing. The prompt-tuning approach [29] reduces the hyperparameter sensitivity, but its performance still remains suboptimal.

To summarize the developments, the following issues persist: 1) Current DINOv2-SAM integration frameworks remain huge, incorporating dual encoders from each model along with SAM’s prompt encoder and mask decoder; 2) DINOv2’s potential is underutilized, being utilized solely for prompt generation; 3) Sparse prompts based on support-query cosine similarity fail to fully exploit the knowledge from the support set. Given these limitations, we wonder *“Is it possible to build a compact encoder-decoder model, but with knowledge from both DINOv2 and SAM?”*

In this work, we build a novel few-shot semantic segmentation (FSSS) model, named FS-DINO, with a unified architecture that includes only the DINOv2 encoder and a lightweight segmenter. Our compact segmenter based on dense prompt of support-query cosine similarity only contains 5M parameters, which is just 5% of SAM’s memory footprint. Upon [17], which is built purely on DINOv2, our segmenter shares similar trainable parameters with it, but incorporates knowledge from SAM via a coarse-to-fine distillation procedure and can be further enhanced by our 4D correlation mining on support-query pairs.

In particular, our segmenter integrates three core modules: a mask decoder, a meta-visual prompt generator, and

an embedding adapter. The first two modules leverage SAM’s prompt-enabled design. Using SAM’s decoder directly is intuitive but challenging due to the distinct feature distributions. SAM’s features typically focus on holistic attention, while DINOv2’s features capture rich details in local regions. Directly distilling features from their last layers does not reduce training loss. To address this, we design a bottleneck adapter upon DINOv2’s 3rd-layer features, which are observed to be most similar to SAM’s embeddings, for coarse-to-fine distillation. Here we train only the adapter while keeping the DINOv2’s encoder fixed to ensure high-quality dense features for prompt generation. By progressively increasing training image resolution from 126×126 to 518×518 , the adapter captures global context before refining local details. Unlike prior works [9, 14] that use geometric prompts of points and boxes, we introduce an automatic Meta-Visual Prompt Generator (MVPG) that directly creates visual prompts to capture comprehensive support-query relationships. Unlike most prior methods that use support as an average vector without spatial information, we introduce an effective module for support-query 4D correlation mining, enhancing the few-shot segmentation significantly. Finally, the meta-visual prompt generator is trained using meta-learning on episodic support-query pairs.

Overall, we summarize our key contributions as follows:

- We introduce a unified framework with a DINOv2 encoder and a lightweight segmenter, significantly reducing footprint compared to dual-model architectures.
- We propose a novel segmenter featuring a bottleneck adapter, meta-visual prompt generator, and mask decoder.
- We develop an effective coarse-to-fine distillation procedure that can integrate SAM’s knowledge into a 1M lightweight adapter.
- We introduce a novel MVPG, providing comprehensive meta-visual prompts and maximizing the mask decoder’s capability.
- Our extensive experiments on widespread datasets have demonstrated the effectiveness of our method.

2. Related Works

Few-shot segmentation Few-shot semantic segmentation (FSSS) aims to segment target objects with a limited number of annotated samples. In this field, meta-learning has been widely adopted to acquire generalized models via episodic training. Early work of [31] constructs prototypes by applying masked average pooling (MAP) to support images and then segments the query image by measuring its pixel-wise distances from prototypes in the metric space. Instead of using a single prototype, [13, 36, 38] represent the same class with multiple prototypes, and [41] used an additional separate encoder to process MAP. Since prototype-based methods are limited by feature av-

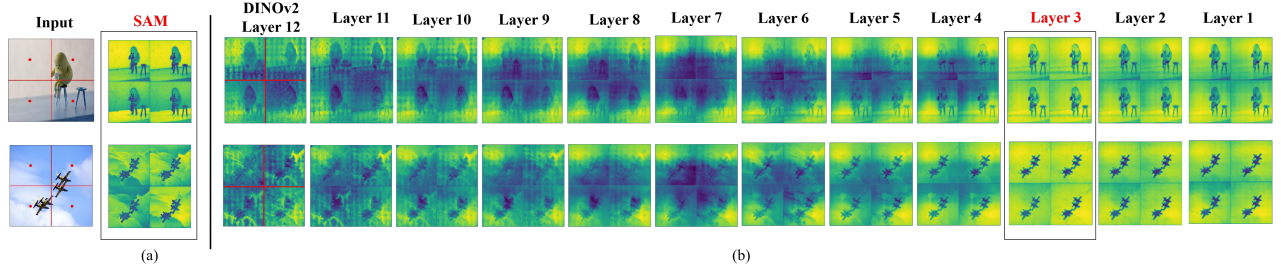


Figure 2. **Analysis on the embeddings from DINOv2 and SAM.** We compute the self-similarity map (SSM) for the feature vectors at the red dot locations to analyze the embedding distribution of both models and visualize them in the figure. Here, (a) shows the SSM of features from the last layer of SAM’s encoder, while (b) displays the SSM of features from all layers of DINOv2-base. Unlike SAM’s holistic semantic focus, DINOv2’s high-level embeddings concentrate on various local regions, offering richer representation. Despite this, we found that embeddings from DINOv2’s 3rd layer are most similar to SAM’s encoder output embeddings. This observation enables efficient cross-model distillation for our lightweight segmenter.

eraging, methods such as [8, 18, 19, 23, 39, 43] explicitly build support-query feature aggregation modules to fully exploit the information in limited support. Among them, [15, 23, 27, 34, 39] employ support-query cross-attentions. Upon the support-query fusion, [16] matches regions to generate a context-aware prior mask. Works such as [8, 23, 27, 43] employ multi-layer features for matching, while [7, 18] compute spatial hyper-correlations between query and support spatial feature maps.

Vision foundation models in few-shot segmentation

With the development of pre-trained visual models such as ViT [3], CLIP [25], SAM [9], and DINOv2 [21], few-shot semantic segmentation (FSSS) models [2, 14, 29] have achieved significant improvements on benchmark datasets. Along with the emergence of SAM and DINO, many methods have explored few-shot segmentation based on them. Since DINO models are trained on 142M images via self-supervised local-to-global distillation that highly respects local correlations, their features turn out to be particularly suitable for segmentation tasks. The training-free method [14] generates point prompts using support-query similarity based on DINOv2 features, with dual-direction pruning. Inspired by [14], [37] enhances segmentation by building a graph on masks derived from point prompts. Other works, like [29], aim to learn prompt encoders to avoid complex hand-crafted procedures but still rely on SAM and DINOv2, resulting in large memory footprints. In contrast, [17] trains a decoder on top of DINOv2, yet lacks integration with SAM’s rich knowledge.

2.1. Preliminary

Since both DINOv2 and SAM are utilized for the few-shot segmentation task [14, 29, 37], the input images are passed through two separate image encoders to extract features independently. This results in a model with a large number of parameters and high inference time, making it less practi-

cal for real-world applications. To address this issue, we propose learning SAM’s feature distribution by introducing a small number of trainable parameters after DINOv2 encoder, enabling SAM’s powerful decoder on top of DINOv2. However, experimental results reveal significant differences between the features from these two models, as illustrated in Figure 2. The distillation loss that aims to align the two kinds of features does not decrease. To this end, we compute self-similarities of features from DINOv2 and SAM’s encoders separately for analysis.

Given a feature representation $F \in \mathbb{R}^{H \times W \times C}$ obtained from the image encoder, we first reshape it into a two-dimensional matrix $F \in \mathbb{R}^{HW \times C}$, and then compute the cosine similarity after normalization, formulated as:

$$S_{ij} = \frac{F_i \cdot F_j}{\|F_i\| \|F_j\|}, \quad \forall i, j \in [1, HW], \quad (1)$$

where S_{ij} represents the similarity between feature vectors at positions i and j . For each position i , by computing its correlation with all positions in the image, we get a similarity map of size $H \times W$. Fig. 2 shows instances of the Self-Similarity Maps (SSM) on several anchor points.

As illustrated in Fig. 2, the self-correlation analysis reveals distinct characteristics between the representations of SAM and DINOv2. SAM’s features exhibit strong global characteristics, where each pixel can perceive semantic information across the entire image. In contrast, DINOv2’s features are more localized, with each pixel focusing primarily on the neighboring regions of the same semantics. *An interesting observation* is that DINOv2 can already capture holistic attention in its early-stage embeddings but is trained to represent richer details in the high-level layers. **This suggests that a full 12-layer model is not strictly necessary for capturing SAM’s representation, and transferring knowledge from DINOv2’s early-stage features is computationally feasible.** Here, we utilize features from the 3rd layer of DINOv2, which are found best matching the distribution of SAM’s output embedding.

3. Method

3.1. Problem Definition

Given a dataset D , it is divided into a training set D_{train} and a test set D_{test} , ensuring no class overlap between the train and test sets, that is $C_{\text{train}} \cap C_{\text{test}} = \emptyset$. A few-shot semantic segmentation (FSSS) model is first trained on the base classes, i.e., the training dataset, and is then directly evaluated on the novel classes, i.e., the test dataset, without further training or fine-tuning. Specifically, given N support images of a novel class c and their masks, the target of the FSSS model is to segment pixels of the class c in a query image conditioned on the supports and their masks, and the process is called N-shot segmentation.

3.2. Model Overview

In this work, we introduce a unified framework consisting of a DINOv2 encoder and a lightweight segmenter, as shown in Fig. 3. In the following, we will give an overview of both our architecture and training strategies.

The Architecture Our segmenter is placed on top of the DINOv2 encoder, and it contains three key components: a bottleneck adapter, a Meta-Visual Prompt Generator (MVPG) and a mask decoder. To take advantage of SAM’s powerful segmentation capability that lies in its decoder, we initialize our decoder with SAM’s pretrained weights. After training, the mask decoder then can segment a query image conditioned on its image embedding from the bottleneck adapter, and the prompts of the target class derived from the MVPG. In particular, the lightweight adapter, taking only 1M parameters, is placed on top of the 3rd layer of DINOv2, and its output embeddings are distilled to match SAM encoder’s output. For the prompts, instead of leveraging geometric prompts in SAM, our MVPG directly generates visual prompts, i.e., the semantic-aware visual prompts and dense prompts based on similarity map, enabling comprehensive support-query relationship modeling and automatic prompting. These two kinds of prompts serve as SAM’s sparse and dense prompts, respectively. Thanks to the bottleneck adapter and MVPG, we are able to establish a unified framework with enhanced decoder.

Training Strategy Our training consists of two stages, i.e., the embedding distillation and training for mask decoding. During both training stages, the DINOv2 encoder is frozen and only parts of our segmenter are trained. In particular, in the first training stage, we train only the adapter with a MSE loss to align the embeddings without being aware of the downstream task. In the second stage, with the DINOv2 encoder and the adapter frozen, the remaining components of the segmenter are further optimized using a meta-learning strategy to enhance few-shot semantic segmentation performance.

3.3. Coarse-to-Fine Distillation for Embedding Alignment

Based on our observation in Sec. 2.1, we directly leverage the 3rd-layer features of DINOv2-base and train a lightweight adapter with a bottleneck structure to align its embeddings with SAM. During the training of embedding distillation, we use the encoder of SAM-ViT-Huge as the teacher, and our adapter on top of DINOv2’s first 3 layers as the student, and only the weights of the adapter are trained.

3.3.1. The Bottleneck Adapter

To maintain a lightweight adapter, we designed a bottleneck-structured module to efficiently transfer embeddings. As shown in Fig. 3, our adapter takes the features from the 3rd layer of DINOv2 as input, denoted as $F_d^3 \in \mathbb{R}^{37 \times 37 \times 768}$, and transfers them to $F_d^{\text{distill}} \in \mathbb{R}^{37 \times 37 \times 256}$ to match the feature dimension from the last layer of the SAM encoder. To this end, we first progressively reduce the feature dimension to 128 by a sequence of convolutions with sizes of $1 \times 1 \times 768 \times 256$, $3 \times 3 \times 256 \times 256$, and $1 \times 1 \times 256 \times 128$. Then we employ two self-attention blocks to process the features, and finally upscale them to dimension 256 via a pointwise convolution. Here, each of the self-attention blocks follows the structure of [30], with the $Q, K, V \in \mathbb{R}^{128 \times 128}$ and inner-layer dimension of the feed-forward network (FFN) being 512.

3.3.2. Cross-modal Distillation from Coarse to Fine

Given the observation that SAM’s features capture holistic semantics, we designed a multi-stage distillation procedure to align the features from coarse to fine. Specifically, we start by distilling using a smaller input size of 126×126 . After each distillation stage, the model continues training based on images of larger resolutions. Our training ends with the resolution of 518×518 , which is the image resolution used by DINOv2. Through this progressive training strategy, our model can gradually fit the feature distribution of SAM, successfully replacing SAM’s image encoder.

Let’s denote by F_d^{distill} the features from our bottleneck adapter, and F_{sam} the features from the last layer of SAM’s encoder. By calculating the mean squared error (MSE) between F_d^{distill} and F_{sam} , we encourage our features to be close to the distribution of SAM encoder’s output. Here we use only 1% of SAM’s training images for feature distillation and training.

3.4. Mask Decoding via Meta-Visual Prompting

Given the image embedding from our bottleneck adapter, we can decode it with our meta-visual prompts for mask prediction. To achieve efficient segmentation with limited labeled images, we employ a meta-training strategy to train Meta-Visual Prompt Generation (MVPG) and the mask decoder.

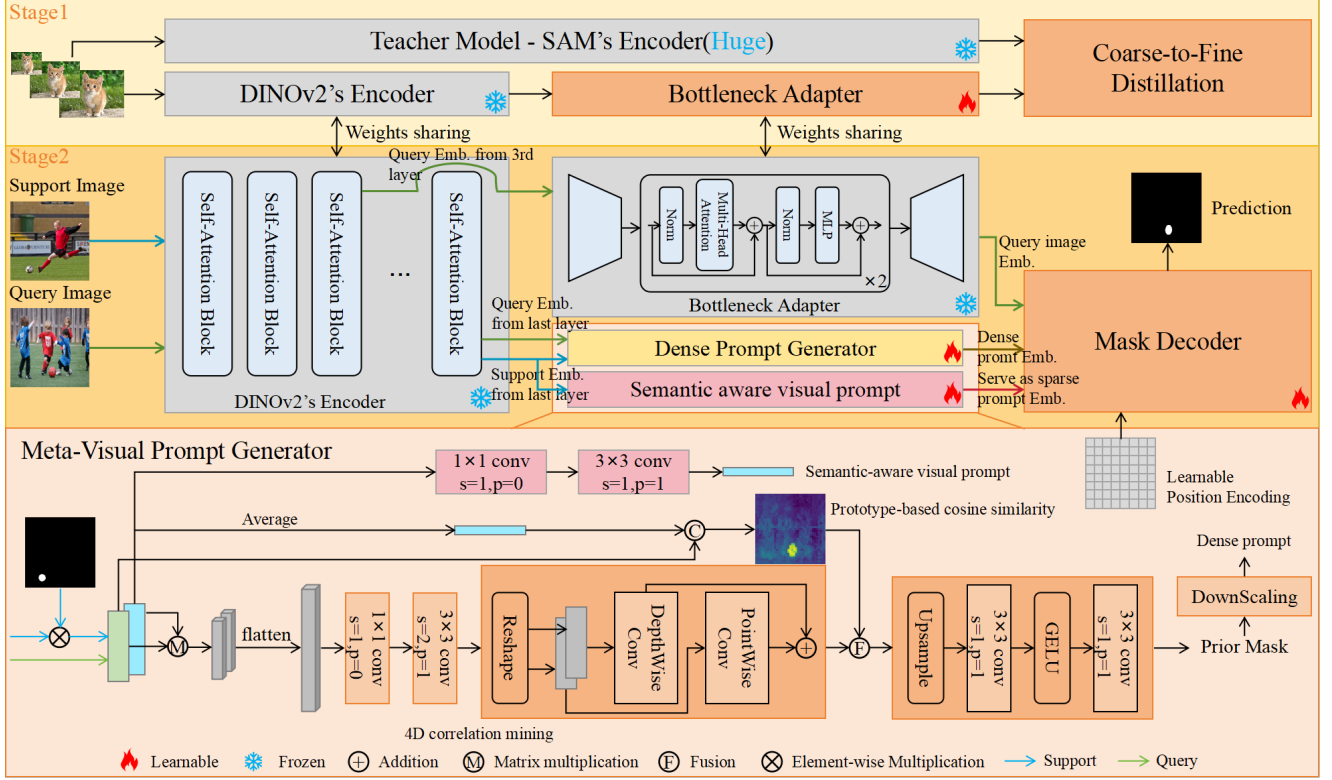


Figure 3. **The proposed FS-DINO Architecture.** Our architecture consists of a DINOv2 encoder and a lightweight segmenter that includes a bottleneck adapter (BA), a Meta-Visual Prompt Generator (MVPG) and a mask decoder. Upper part is the coarse-to-fine cross-model distillation procedure, with only the adapter trainable for feature matching. Below is the overall architecture of our few-shot semantic segmentation model. Our MVPG includes three modules for multiple kinds of prompts, which are (a) the semantic-aware visual prompts, (b) dense prompts of direct cosine similarity between the support and query, and (c) dense prompts of support-query 4D correlation.

3.4.1. Meta-Visual Prompt Generator

For interactive prompting, SAM requires sparse and dense prompts for segmentation, with sparse prompts of points and boxes typically provided by human annotators. Unlike SAM’s interactive manner and prior FSSS methods [14, 37] that use geometric sparse prompts, we directly generate visual prompts for automatic prompting.

Semantic-aware Visual Prompts For the sparse prompts, we directly generate a vector of embedding based on the support features. In particular, we process the support features from DINOv2’s last layer to match the dimension of SAM’s sparse prompt embedding, and then average them to a vector with dimension 256.

Dense Prompts of Prototype-based Cosine Similarity

Let’s denote $F_s \in \mathbb{R}^{H \times W \times C}$ and $F_q \in \mathbb{R}^{H \times W \times C}$ the support and query features from the last layer of DINOv2 encoder. We apply Mean Aggregation Pooling (MAP) to the support feature F_s , to obtain the prototype $p \in \mathbb{R}^{1 \times C}$ on the support class c . The cosine similarity map between the class prototype p and the query feature map F_q can be

calculated as follows:

$$S_{pcs}(i, j) = \frac{p \cdot F_q^T(i, j)}{\|p\| \|F_q(i, j)\|}, \quad p = \frac{1}{HW} \sum_{i=1}^H \sum_{j=1}^W F_s(i, j), \quad (2)$$

where $F_s(i, j)$ and $F_q(i, j)$ represent support and query feature vectors at location (i, j) , respectively. S_{pcs} is the similarity map of size $[H, W]$, which serves as dense prompt for mask decoding. Note that the process of computing S_{pcs} is parameter-free. *A compact version of our framework, which encompasses MVPG based on solely S_{pcs} and the semantic-aware visual prompts, introduces only 5M parameters upon DINOv2, but achieves competitive performance on FSSS tasks.*

Dense Prompts of 4D Correlations Since directly using the prototype-based similarity map as the dense prompt fails to fully exploit the information contained in the support features, we compute the 4D dense correlation between the support feature F_s and the query feature F_q via a matrix multiplication, which is formulated as,

$$S_{4d} = F_q F_s^T, \quad S_{4d} \in \mathbb{R}^{H_q \times W_q \times H_s \times W_s}. \quad (3)$$

By iteratively processing on support and query dimensions, the proposed module completes knowledge aggregation and fusion on the hypercorrelation.

For efficient training, we first downsample S_{4d} to a smaller size and then process the 4D correlation in a low-dimensional space. In particular, by flattening S_{4d} , it is reshaped to size $H_q \times W_q \times H_s W_s$, where both the width and height of the support and query are 37. Here each vector on the query unfolds its correlation to the whole support image. Its dimension is then gradually reduced by two convolutions of size $1 \times 1 \times 1369 \times 512$ and $3 \times 3 \times 512 \times 361$, with the latter taking stride 2, resulting in a new dense correlation of size $\lceil H_q/2 \rceil \times \lceil H_q/2 \rceil \times \lceil H_s/2 \rceil \lceil W_s/2 \rceil$. Through convolution and dimension reduction, information on the support dimension is also exchanged and fused.

Afterwards, we reshape the dense 4D correlation [18] into two forms, S_{4d}^1 and S_{4d}^2 , by flattening and transposing operations, where $S_{4d}^1 \in \mathbb{R}^{\lceil \frac{H_q}{2} \rceil \times \lceil \frac{W_q}{2} \rceil \times \lceil \frac{H_s}{2} \rceil \lceil \frac{W_s}{2} \rceil}$, $S_{4d}^2 \in \mathbb{R}^{\lceil \frac{H_s}{2} \rceil \times \lceil \frac{W_s}{2} \rceil \times \lceil \frac{H_q}{2} \rceil \lceil \frac{W_q}{2} \rceil}$. The two matrices are then processed via depthwise and pointwise convolutions to enable information interaction while avoiding high-dimensional computation,

$$\hat{S}_{4d}^1 = \text{Depthwise_conv}(S_{4d}^1), \quad (4)$$

$$\hat{S}_{4d}^2 = \text{Pointwise_conv}(S_{4d}^2). \quad (5)$$

To capture the spatial structure of the query more efficiently, depthwise convolution with 3×3 kernel is applied on \hat{S}_{4d}^1 . On the other hand, pointwise convolution is applied to \hat{S}_{4d}^2 to strengthen the relationship between points at different positions in the query. Then, both \hat{S}_{4d}^1 and \hat{S}_{4d}^2 are reshaped and added together, resulting in $\hat{S}_{4d} \in \mathbb{R}^{\lceil \frac{H_q}{2} \rceil \times \lceil \frac{W_q}{2} \rceil \times \lceil \frac{H_s}{2} \rceil \lceil \frac{W_s}{2} \rceil}$. We then perform a per-channel addition between \hat{S}_{4d} and the prototype-based similarity map S_{pcs} to achieve a more reliable correlation map \hat{S}_{4d}^n .

The correlation map \hat{S}_{4d}^n is then subsequently upsampled via a series of 3×3 convolutions to a resolution of $4 \times$ higher and downsampled to a single channel. Despite upsampling, this process effectively fuses correlations on support maps. In the end, we obtain a prior mask $P_{prior.m}$, which is a score map for the target category. The prior mask will be supervised during training for improved performance. The dense prompt embedding will be obtained after downscaling through the original SAM module.

3.4.2. Mask Decoder for Novel Class Segmentation

To segment novel classes in the query image, we leverage a mask decoder to decode the target regions based on the image embedding of our bottleneck adapter, with the joint guidance of the dense prompt and the semantic-aware visual prompt. Furthermore, during training, we introduce a learnable positional encoding based on a Gaussian matrix, which

is derived from random Fourier features, to encode positional information of the training data into the model. This operation helps the mask decoder better distinguish pixels.

3.4.3. Episodic Training for Mask Decoding

Episodic training is a common training strategy designed to simulate the inference process, enabling the model to generalize effectively to unseen classes. In each training iteration, the model processes several support-query pairs and predicts the query mask for the target class, which is the class of the corresponding support sample in the pair.

During our training for mask decoding, we employ the episodic training strategy to train the segmenter. For the mask decoder, we initialize its parameters with those from the pre-trained mask decoder of SAM-ViT-Huge. It is important to note that during episodic training, we train exclusively on the base classes without involving the novel classes. The Dice Loss and BCE Loss are computed separately for the prior mask $P_{prior.m}$ and the final prediction P_m against the ground truth M_q . Particularly, the loss functions are defined as:

$$\mathcal{L}_{prior} = \mathcal{L}_{Dice}(P_{prior.m}, M_q) + \mathcal{L}_{BCE}(P_{prior.m}, M_q) \quad (6)$$

$$\mathcal{L}_{final} = \mathcal{L}_{Dice}(P_m, M_q) + \mathcal{L}_{BCE}(P_m, M_q) \quad (7)$$

$$\mathcal{L} = \mathcal{L}_{prior} + \mathcal{L}_{final} \quad (8)$$

where $\mathcal{L}_{Dice}(\cdot)$ and $\mathcal{L}_{BCE}(\cdot)$ represent the Dice Loss and Binary Cross-Entropy (BCE) Loss, respectively.

4. Experiments

To evaluate the effectiveness of our proposed method, we conducted extensive experiments on two widely recognized benchmark datasets in the Few-Shot Semantic Segmentation (FSSS) setting: PASCAL-5i [26] and COCO-20i [20]. The PASCAL-5i dataset, derived from PASCAL VOC 2012 [4], is augmented with additional annotations from SDS [5] and consists of 20 object categories, including an auxiliary "background" class. The COCO-20i dataset, constructed from MSCOCO [12], presents a more challenging setting as it includes 80 categories, also with a "background" class. In addition, we test in an out-of-distribution setting, where we train the model on COCO-20i base datasets, and directly test the model on the test set of FSS-1000 and DAVIS-17 datasets. Here the FSS-1000 [11] is a dataset designed specifically for FSSS with 1000 categories, and DAVIS-17 [24] is a dataset tailored for video segmentation which contains 20 videos for testing.

4.1. Implementation Details

The lightweight Bottleneck Adapter(BA) is trained on 1% of the SA-1B dataset [9] with three stages. In each stage, we train the model for 15 epochs, using an image size of

Method	backbone	1-shot					5-shot				
		Fold0	Fold1	Fold2	Fold3	Mean	Fold0	Fold1	Fold2	Fold3	Mean
BAM ^{CVPR'22} [10]	ResNet50	69.0	73.6	67.6	61.1	67.8	70.6	75.1	70.8	67.2	70.9
HDMNet ^{CVPR'23} [23]		71.0	75.4	68.9	62.1	69.4	71.3	76.2	71.3	68.5	71.8
AENet ^{ECCV'24} [35]		71.3	75.9	68.6	65.4	70.3	73.9	77.8	73.3	72.0	74.2
MSI ^{ICCV'23} [19]	ResNet101	73.1	73.9	64.7	68.8	70.1	73.6	76.1	68.0	71.3	72.2
SCCAN ^{ICCV'23} [34]		70.9	73.9	66.8	61.7	68.3	73.1	76.4	70.3	66.1	71.5
ABCB ^{CVPR'24} [42]		73.0	76.0	69.7	69.2	72.0	74.8	78.5	73.6	72.6	74.9
Matcher ^{ICLR'24} [14]	DINOv2-L, SAM-H	67.7	70.7	66.9	67.0	68.1	71.4	77.5	74.1	72.8	74.0
GF-SAM ^{NeurIPS'24} [37]		71.1	75.7	69.2	73.3	72.1	81.5	86.3	79.7	82.9	82.6
VRP-SAM ^{CVPR'24} [29]	ResNet50, SAM-H	73.9	<u>78.3</u>	70.6	65.0	71.9	-	-	-	-	-
FCP ^{AAAI'25} [22]		<u>74.9</u>	77.4	<u>71.8</u>	<u>68.8</u>	<u>73.2</u>	<u>77.2</u>	<u>78.8</u>	<u>72.2</u>	<u>67.7</u>	<u>74.0</u>
Ours	DINOv2-B	75.6	80.3	72.2	73.4	75.4	78.1	83.1	73.6	76.3	77.8

Table 1. Performance comparisons on PASCAL-5i under 1-shot and 5-shot settings. Results in bold indicate the best performance, and results with underlining represent the second-best performance.

Method	backbone	1-shot					5-shot				
		Fold0	Fold1	Fold2	Fold3	Mean	Fold0	Fold1	Fold2	Fold3	Mean
BAM ^{CVPR'22} [10]	ResNet50	43.4	50.6	47.5	43.4	46.2	49.3	54.2	51.6	49.6	51.2
HDMNet ^{CVPR'23} [23]		43.8	55.3	51.6	49.4	50.0	50.6	61.6	55.7	56.0	56.0
AENet ^{ECCV'24} [35]		45.4	57.1	52.6	50.0	51.3	52.7	62.6	56.8	56.1	57.1
MSI ^{ICCV'23} [19]	ResNet101	44.8	54.2	52.3	48.0	49.8	49.3	58.0	56.1	52.7	54.0
SCCAN ^{ICCV'23} [34]		42.6	51.4	50.0	48.8	48.2	49.4	61.7	61.9	55.0	57.0
ABCB ^{CVPR'24} [42]		46.0	56.3	54.3	51.3	51.5	51.6	63.5	62.8	57.2	58.8
Matcher ^{ICLR'24} [14]	DINOv2-L, SAM-H	52.7	53.5	52.6	52.1	52.7	60.1	62.7	60.9	59.2	60.7
GF-SAM ^{NeurIPS'24} [37]		56.6	61.4	59.6	57.1	58.7	67.1	69.4	66.0	64.8	66.8
FCP ^{AAAI'25} [22]	ResNet50, SAM-H	46.4	56.4	55.3	51.8	52.5	<u>52.6</u>	<u>63.3</u>	<u>59.8</u>	<u>56.1</u>	<u>58.0</u>
VRP-SAM ^{CVPR'24} [29]	DINOv2-B, SAM-H	<u>56.8</u>	<u>61.0</u>	64.2	<u>59.7</u>	<u>60.4</u>	-	-	-	-	-
SEGIC ^{ECCV'24} [17]	DINOv2-B	55.8	54.7	52.4	51.4	53.6	-	-	-	-	-
Ours	DINOv2-B	58.6	66.0	<u>62.3</u>	62.6	62.4	62.1	70.2	66.1	63.0	65.4

Table 2. Performance comparisons on COCO-20i under 1-shot and 5-shot settings. We achieved the best results compared to methods that also are based on DINOv2-base. Our model also gains competitive performance compared to heavy architecture based on DINOv2-large (DINOv2-L) and SAM-Huge (SAM-H), especially under 1-shot setting.

Method	backbone	FSS-1000	DAVIS-17
		mIoU	$\mathcal{J}\&\mathcal{F}$
Painter [32]	ViT-L	61.7	34.6
SegGPT [33]	ViT-L	85.6	50.0
PerSAM [†] [40]	ViT-H	71.2	60.3
PerSAM-F [†] [40]	ViT-H	75.6	71.9
Matcher [†] [14]	ViT-H+ViT-G	33.0	79.5
SegIC [17]	ViT-L	86.8	71.4
Ours	ViT-B	87.2	76.6

Table 3. Performance comparisons on FSS-1000 and DAVIS-17 under one-shot setting. The $\mathcal{J}\&\mathcal{F}$ indicates the combination of the Jaccard index (J) for overlap and the F1-score (F) for precision and recall balance.

126×126, 252×252, and 518×518, respectively. In the first two stages, the model is trained on 2 NVIDIA RTX A6000, and in the last stage on 4 RTX A6000 GPUs, with a batch

BA	SVP	PCS	4D Corr.	mIoU (%)	FB-IoU (%)
✓		✓		58.2	77.2
✓	✓	✓		59.6	77.3
✓	✓	✓	✓	62.4	79.0

Table 4. Ablation study results on COCO-20i under the one-shot setting. Here, we denote BA as the Bottleneck Adapter, SVP the Semantic Visual Prompt, PCS the Prototype-based Cosine Similarity, and 4D Corr. the Dense Prompts based on 4D correlation mining.

size of 8 and an initial learning rate of 0.001.

While training for mask decoding and few-shot segmentation, all experiments on the PASCAL-5i [26] and COCO-20i [20] datasets were conducted with images of size 518×518 pixels, using the DINOv2 pre-trained model ViT-B/16. All the experiments were implemented on a sin-

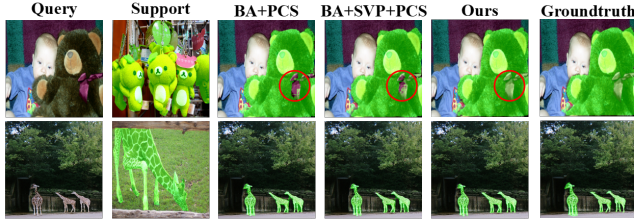


Figure 4. Qualitative results of the proposed method.

gle NVIDIA A6000 GPU. To ensure fairness in comparisons, we used the same data augmentations, optimizer and learning rate with [23]. That is, AdamW was used as the optimizer with a learning rate of 0.001, and the batch size is set to 8 for both the PASCAL-5i and COCO-20i datasets. Regarding optimization and scheduling, the model was trained with an episodic training scheme for 100 and 50 epochs on the PASCAL-5i and COCO-20i datasets, respectively.

4.2. Comparison with State-of-the-Art Methods

Few-shot Segmentation Performance. Table 1 presents a comparative evaluation of our method against state-of-the-art approaches on PASCAL-5i under both 1-shot and 5-shot settings. In the 1-shot scenario, our method exhibits a significant performance boost, outperforming FCP [22] by 2.2% and GF-SAM [37] by 3.3% in mIoU. Notably, our model only utilizes DINOv2-base [21], the SAM [9] mask decoder, and a minimal set of trainable parameters, thereby substantially reducing model size and training overhead compared to approaches leveraging SAM-H and DINOv2-large. Under the 5-shot setting, our method consistently surpasses most existing approaches, achieving mIoU improvements of 3.8% over FCP [22].

Table 2 reports the results on COCO-20i, further substantiating the effectiveness of our approach. In the 1-shot setting, our method attains state-of-the-art performance, with mIoU gains of 5.5% over GF-SAM [37] and 8.8% over SEGIC [17]. In the 5-shot setting, our approach continues to outperform most existing methods, surpassing Matcher [14] by 4.7% and FCP [22] by 7.4%.

Out-of-Distribution Performance To evaluate the generalizability of our model, we perform one-shot assessments on the FSS-1000 and DAVIS-17 datasets [24] following [17]. It is important to note that we directly applied a model pretrained on the COCO-20i base set to these datasets without any additional fine-tuning. This setting is specifically challenging due to the significant domain shifts between the datasets. The results are presented in Tab. 3. As shown in the table, our model surpasses SEGIC [17] and PerSAM-F[†] [40], demonstrating outstanding transferability.

4.3. Ablation study

To evaluate our model’s effectiveness, we conducted thorough ablation studies on COCO-20i under the one-shot setting. To maintain experimental consistency, we selected DINOv2-base as the image encoder and trained the mask decoder for novel-class segmentation. These experiments systematically analyze our model’s performance across different conditions. The results are shown in Tab. 4.

Bottleneck Adapter To verify the effectiveness of our proposed Bottleneck Adapter (BA), we leverage the features of the bottleneck adapter from the final distillation stage as the image embedding for mask decoding. The dense prompt for the mask decoder is derived solely through Prototype-based Cosine Similarity (PCS), effectively guiding the segmentation of the target object. When comparing our results achieved by *BA+PCS* with Matcher [14], our model can achieve a 5.5% performance improvement over [14], which serves as a benchmark for FSSS based on DINOv2-large and SAM-H. This strongly demonstrates the superiority of our architecture and the effectiveness of the proposed coarse-to-fine distillation strategy.

Semantic-aware Visual Prompts For mask decoding, we introduce learnable positional encodings and transform the masked support features to serve as the mask decoder’s sparse prompts, while removing the original prompt encoder from SAM. An interesting observation is that, using initial sparse prompt embedding from SAM can also lead to competitive results, as shown by *BA+PCS*. By replacing the initial sparse embedding with our trainable semantic-aware vision prompts (SVP), we gained 1.4% improvement on mIoU. Note that, the model shown by *BA+SVP+PCS* is also our compact version with only 5M parameters upon DINOv2. The performance of this model is quite competitive, outperforming strong baselines, such as SEGIC [17], FCP [22] and even GF-SAM [37] that relies on large ViTs.

Dense Prompts of 4D Correlations Upon the model with Bottle Adapter (BA) and Semantic-aware Visual Prompts (SVP), we get a significant performance improvement of 2.8% mIoU by introducing the dense prompts of 4D correlation (4D Corr.), as shown by *BA+SVP+PCS+4D Corr.* in Tab. 4. Our module for 4D correlation is efficient with only 4M parameters, helping maintain the overall lightweight nature of the segmenter.

Visualized results shown in Fig. 4 show that each our design contributes to the final improvements, leading to accurate segmentation on novel classes.

5. Conclusion

In this work, we utilize vision foundation models for few-shot segmentation, finding that DINOv2 features offer strong discriminability across classes. This enables the generation of accurate prior information to guide the

segmentation process. To enhance efficiency and accelerate inference, we design a lightweight bottleneck adapter on the third-layer features of DINOv2’s image encoder, which learns from SAM’s encoder through coarse-to-fine distillation. Additionally, we propose a meta-visual prompt generator that leverages the capabilities of large-scale pre-trained models and serves for SAM’s mask decoder for complete decoding. Extensive experiments demonstrate the effectiveness of our model. Our future work will explore further improvements in accuracy and generalization.

References

- [1] Mathilde Caron, Hugo Touvron, Ishan Misra, Hervé Jégou, Julien Mairal, Piotr Bojanowski, and Armand Joulin. Emerging properties in self-supervised vision transformers. In *Proceedings of the IEEE/CVF international conference on computer vision*, pages 9650–9660, 2021. 2
- [2] Shuai Chen, Fanman Meng, Runtong Zhang, Heqian Qiu, Hongliang Li, Qingbo Wu, and Linfeng Xu. Visual and textual prior guided mask assemble for few-shot segmentation and beyond. *IEEE Transactions on Multimedia*, 26:7197–7209, 2024. 3
- [3] Alexey Dosovitskiy, Lucas Beyer, Alexander Kolesnikov, Dirk Weissenborn, Xiaohua Zhai, Thomas Unterthiner, Mostafa Dehghani, Matthias Minderer, Georg Heigold, Sylvain Gelly, et al. An image is worth 16x16 words: Transformers for image recognition at scale. *arXiv preprint arXiv:2010.11929*, 2020. 3
- [4] Mark Everingham, Luc Van Gool, Christopher KI Williams, John Winn, and Andrew Zisserman. The pascal visual object classes (voc) challenge. *International journal of computer vision*, 88:303–338, 2010. 6
- [5] Bharath Hariharan, Pablo Arbeláez, Lubomir Bourdev, Subhransu Maji, and Jitendra Malik. Semantic contours from inverse detectors. In *2011 international conference on computer vision*, pages 991–998. IEEE, 2011. 6
- [6] Weizhao He, Yang Zhang, Wei Zhuo, Linlin Shen, Jiaqi Yang, Songhe Deng, and Liang Sun. Apseg: auto-prompt network for cross-domain few-shot semantic segmentation. In *Proceedings of the IEEE/CVF Conference on Computer Vision and Pattern Recognition*, pages 23762–23772, 2024. 2
- [7] Sunghwan Hong, Seokju Cho, Jisu Nam, Stephen Lin, and Seungryong Kim. Cost aggregation with 4d convolutional swin transformer for few-shot segmentation. In *European Conference on Computer Vision*, pages 108–126. Springer, 2022. 2, 3
- [8] Ehtesham Iqbal, Sirojbek Safarov, and Seongdeok Bang. Msanet: Multi-similarity and attention guidance for boosting few-shot segmentation. *arXiv preprint arXiv:2206.09667*, 2022. 2, 3
- [9] Alexander Kirillov, Eric Mintun, Nikhila Ravi, Hanzi Mao, Chloe Rolland, Laura Gustafson, Tete Xiao, Spencer Whitehead, Alexander C Berg, Wan-Yen Lo, et al. Segment anything. In *Proceedings of the IEEE/CVF international conference on computer vision*, pages 4015–4026, 2023. 2, 3, 6, 8
- [10] Chunbo Lang, Gong Cheng, Binfei Tu, and Junwei Han. Learning what not to segment: A new perspective on few-shot segmentation. In *Proceedings of the IEEE/CVF conference on computer vision and pattern recognition*, pages 8057–8067, 2022. 7
- [11] Xiang Li, Tianhan Wei, Yau Pun Chen, Yu-Wing Tai, and Chi-Keung Tang. Fss-1000: A 1000-class dataset for few-shot segmentation. In *Proceedings of the IEEE/CVF conference on computer vision and pattern recognition*, pages 2869–2878, 2020. 6
- [12] Tsung-Yi Lin, Michael Maire, Serge Belongie, James Hays, Pietro Perona, Deva Ramanan, Piotr Dollár, and C Lawrence Zitnick. Microsoft coco: Common objects in context. In *Computer vision—ECCV 2014: 13th European conference, zurich, Switzerland, September 6–12, 2014, proceedings, part v 13*, pages 740–755. Springer, 2014. 6
- [13] Yongfei Liu, Xiangyi Zhang, Songyang Zhang, and Xuming He. Part-aware prototype network for few-shot semantic segmentation. In *Computer Vision—ECCV 2020: 16th European Conference, Glasgow, UK, August 23–28, 2020, Proceedings, Part IX 16*, pages 142–158. Springer, 2020. 2
- [14] Yang Liu, Muzhi Zhu, Hengtao Li, Hao Chen, Xinlong Wang, and Chunhua Shen. Matcher: Segment anything with one shot using all-purpose feature matching. *arXiv preprint arXiv:2305.13310*, 2023. 1, 2, 3, 5, 7, 8
- [15] Zhihe Lu, Sen He, Xiatian Zhu, Li Zhang, Yi-Zhe Song, and Tao Xiang. Simpler is better: Few-shot semantic segmentation with classifier weight transformer. In *Proceedings of the IEEE/CVF International Conference on Computer Vision*, pages 8741–8750, 2021. 3
- [16] Xiaoli Luo, Zhuotao Tian, Taiping Zhang, Bei Yu, Yuan Yan Tang, and Jiaya Jia. Pfenet++: Boosting few-shot semantic segmentation with the noise-filtered context-aware prior mask. *IEEE Transactions on Pattern Analysis and Machine Intelligence*, 46(2):1273–1289, 2023. 3
- [17] Lingchen Meng, Shiyi Lan, Hengduo Li, Jose M Alvarez, Zuxuan Wu, and Yu-Gang Jiang. Segic: Unleashing the emergent correspondence for in-context segmentation. In *European Conference on Computer Vision*, pages 203–220. Springer, 2024. 2, 3, 7, 8
- [18] Juhong Min, Dahyun Kang, and Minsu Cho. Hypercorrelation squeeze for few-shot segmentation. In *Proceedings of the IEEE/CVF international conference on computer vision*, pages 6941–6952, 2021. 2, 3, 6
- [19] Seonghyeon Moon, Samuel S Sohn, Honglu Zhou, Sejong Yoon, Vladimir Pavlovic, Muhammad Haris Khan, and Mubbasir Kapadia. Msi: Maximize support-set information for few-shot segmentation. In *Proceedings of the IEEE/CVF International Conference on Computer Vision*, pages 19266–19276, 2023. 3, 7
- [20] Khoi Nguyen and Sinisa Todorovic. Feature weighting and boosting for few-shot segmentation. In *Proceedings of the IEEE/CVF international conference on computer vision*, pages 622–631, 2019. 6, 7
- [21] Maxime Oquab, Timothée Darcet, Théo Moutakanni, Huy Vo, Marc Szafraniec, Vasil Khalidov, Pierre Fernandez,

- Daniel Haziza, Francisco Massa, Alaaeldin El-Nouby, et al. Dinov2: Learning robust visual features without supervision. *arXiv preprint arXiv:2304.07193*, 2023. 2, 3, 8
- [22] Suho Park, SuBeen Lee, Hyun Seok Seong, Jaejoon Yoo, and Jae-Pil Heo. Foreground-covering prototype generation and matching for sam-aided few-shot segmentation. *arXiv preprint arXiv:2501.00752*, 2025. 7, 8
- [23] Bohao Peng, Zhuotao Tian, Xiaoyang Wu, Chengyao Wang, Shu Liu, Jingyong Su, and Jiaya Jia. Hierarchical dense correlation distillation for few-shot segmentation. In *Proceedings of the IEEE/CVF Conference on Computer Vision and Pattern Recognition*, pages 23641–23651, 2023. 2, 3, 7, 8
- [24] Jordi Pont-Tuset, Federico Perazzi, Sergi Caelles, Pablo Arbeláez, Alex Sorkine-Hornung, and Luc Van Gool. The 2017 davis challenge on video object segmentation. *arXiv preprint arXiv:1704.00675*, 2017. 6, 8
- [25] Alec Radford, Jong Wook Kim, Chris Hallacy, Aditya Ramesh, Gabriel Goh, Sandhini Agarwal, Girish Sastry, Amanda Askell, Pamela Mishkin, Jack Clark, et al. Learning transferable visual models from natural language supervision. In *International conference on machine learning*, pages 8748–8763. PmLR, 2021. 2, 3
- [26] Amirreza Shaban, Shray Bansal, Zhen Liu, Irfan Essa, and Byron Boots. One-shot learning for semantic segmentation. *arXiv preprint arXiv:1709.03410*, 2017. 1, 6, 7
- [27] Xinyu Shi, Dong Wei, Yu Zhang, Donghuan Lu, Munan Ning, Jiashun Chen, Kai Ma, and Yefeng Zheng. Dense cross-query-and-support attention weighted mask aggregation for few-shot segmentation. In *European Conference on Computer Vision*, pages 151–168. Springer, 2022. 3
- [28] Jake Snell, Kevin Swersky, and Richard Zemel. Prototypical networks for few-shot learning. *Advances in neural information processing systems*, 30, 2017. 1
- [29] Yanpeng Sun, Jiahui Chen, Shan Zhang, Xinyu Zhang, Qiang Chen, Gang Zhang, Errui Ding, Jingdong Wang, and Zechao Li. Vrp-sam: Sam with visual reference prompt. In *Proceedings of the IEEE/CVF Conference on Computer Vision and Pattern Recognition*, pages 23565–23574, 2024. 1, 2, 3, 7
- [30] Ashish Vaswani, Noam Shazeer, Niki Parmar, Jakob Uszkoreit, Llion Jones, Aidan N Gomez, Łukasz Kaiser, and Illia Polosukhin. Attention is all you need. *Advances in neural information processing systems*, 30, 2017. 4
- [31] Kaixin Wang, Jun Hao Liew, Yingtian Zou, Daquan Zhou, and Jiashi Feng. Panet: Few-shot image semantic segmentation with prototype alignment. In *proceedings of the IEEE/CVF international conference on computer vision*, pages 9197–9206, 2019. 1, 2
- [32] Xinlong Wang, Wen Wang, Yue Cao, Chunhua Shen, and Tiejun Huang. Images speak in images: A generalist painter for in-context visual learning. In *Proceedings of the IEEE/CVF Conference on Computer Vision and Pattern Recognition*, pages 6830–6839, 2023. 7
- [33] Xinlong Wang, Xiaosong Zhang, Yue Cao, Wen Wang, Chunhua Shen, and Tiejun Huang. Seggpt: Towards segmenting everything in context. In *Proceedings of the IEEE/CVF International Conference on Computer Vision*, pages 1130–1140, 2023. 7
- [34] Qianxiong Xu, Wenting Zhao, Guosheng Lin, and Cheng Long. Self-calibrated cross attention network for few-shot segmentation. In *Proceedings of the IEEE/CVF international conference on computer vision*, pages 655–665, 2023. 3, 7
- [35] Qianxiong Xu, Guosheng Lin, Chen Change Loy, Cheng Long, Ziyue Li, and Rui Zhao. Eliminating feature ambiguity for few-shot segmentation. In *European Conference on Computer Vision*, pages 416–433. Springer, 2024. 7
- [36] Boyu Yang, Chang Liu, Bohao Li, Jianbin Jiao, and Qixiang Ye. Prototype mixture models for few-shot semantic segmentation. In *Computer Vision–ECCV 2020: 16th European Conference, Glasgow, UK, August 23–28, 2020, Proceedings, Part VIII 16*, pages 763–778. Springer, 2020. 2
- [37] Anqi Zhang, Guangyu Gao, Jianbo Jiao, Chi Liu, and Yunchao Wei. Bridge the points: Graph-based few-shot segment anything semantically. *Advances in Neural Information Processing Systems*, 37:33232–33261, 2025. 1, 2, 3, 5, 7, 8
- [38] Bingfeng Zhang, Jimin Xiao, and Terry Qin. Self-guided and cross-guided learning for few-shot segmentation. In *Proceedings of the IEEE/CVF conference on computer vision and pattern recognition*, pages 8312–8321, 2021. 2
- [39] Gengwei Zhang, Guoliang Kang, Yi Yang, and Yunchao Wei. Few-shot segmentation via cycle-consistent transformer. *Advances in Neural Information Processing Systems*, 34:21984–21996, 2021. 2, 3
- [40] Renrui Zhang, Zhengkai Jiang, Ziyu Guo, Shilin Yan, Junting Pan, Xianzheng Ma, Hao Dong, Peng Gao, and Hongsheng Li. Personalize segment anything model with one shot. *arXiv preprint arXiv:2305.03048*, 2023. 2, 7, 8
- [41] Xiaolin Zhang, Yunchao Wei, Yi Yang, and Thomas S Huang. Sg-one: Similarity guidance network for one-shot semantic segmentation. *IEEE transactions on cybernetics*, 50(9):3855–3865, 2020. 2
- [42] Lanyun Zhu, Tianrun Chen, Jianxiong Yin, Simon See, and Jun Liu. Addressing background context bias in few-shot segmentation through iterative modulation. In *Proceedings of the IEEE/CVF conference on computer vision and pattern recognition*, pages 3370–3379, 2024. 7
- [43] Yunzhi Zhuge and Chunhua Shen. Deep reasoning network for few-shot semantic segmentation. In *Proceedings of the 29th ACM International Conference on Multimedia*, pages 5344–5352, 2021. 3